ISSN 1392–1320 MATERIALS SCIENCE (MEDŽIAGOTYRA). Vol. 19, No. 4. 2013

# Kinetics of the Thermal Degradation of Granulated Scrap Tyres: a Model-free Analysis

**Félix A. LÓPEZ** [1] *, **Amir A. EL HADAD** [2], **Francisco J. ALGUACIL** [1], **Teresa A. CENTENO** [3], **Belén LOBATO** [3]

[1] *Centro Nacional de Investigaciones Metalúrgicas CENIM (CSIC), Avda. Gregorio del Amo 8, E-28040 Madrid, Spain*
[2] *School of Science and Technology, Nottingham Trent University, Clifton Lane, Nottingham, NG11 8NS, U.K*
[3] *Instituto Nacional del Carbón INCAR (CSIC), Apartado 73, 33080 Oviedo, Spain*

http://dx.doi.org/10.5755/j01.ms.19.4.2947

*Received 28 November 2012; accepted 01 August 2013*

Pyrolysis is a technology with a promising future in the recycling of scrap tyres. This paper determines the thermal decomposition behaviour and kinetics of granulated scrap tyres (GST) by examining the thermogravimetric/derivative thermogravimetric (TGA/DTG) data obtained during their pyrolysis in an inert atmosphere at different heating rates. The model-free methods of Friedman, Flynn-Wall-Ozawa and Coats-Redfern were used to determine the reaction kinetics from the DTG data. The apparent activation energy and pre-exponential factor for the degradation of GST were calculated. A comparison with the results obtained by other authors was made.

*Keywords*: granulated scrap tyre, TGA/DTG, kinetic, pyrolysis.

## 1. INTRODUCTION

Every year about 3.2 million tonnes of end-of-life tyres (ELTs) are generated in the European Union, of which 2.5 million tonnes are either recycled or recovered (10 % reused; 8 % retreaded; 40 % material recovered; 38 % energy recovered) and some 0.7 million tonnes are dumped in landfills [1]. However, the high volatile compound content and the gross calorific value (GCV) of ELTs (33 MJ/kg – 35 MJ/kg) make the recovery of energy from this material an attractive recycling option [2].

Tyres are usually made of different rubbers, including natural rubber (NR), butadiene rubber (BR) and styrene-butadiene rubber (SBR), along with other synthetic polymers, carbon black, and some organic additives. Pyrolysis (thermal degradation in the absence of oxygen) is one of the main techniques used in their recycling. This converts their organic matter into non-condensable gases, a ondensable liquid (tyre-derived oil [TDO]), and a solid residue (tyre-derived char [TDC]).

The quality and quantity of these fractions depend greatly on the composition of the scrap tyres pyrolysed, but also on the design of the reactor in which the pyrolysis takes place and the temperature at which it is performed. At temperatures of around 500 °C – 550 °C the major product is a TDO containing different hydrocarbons, whereas above 650 °C – 700°C the main product is a gas, the result of the further cracking of the liquid fraction [3].

Thermogravimetric analysis (TGA) and derivative thermogravimetry (DTG) are common technique used to measure the mass loss kinetics associated with the vaporization of materials during pyrolysis [4]. Some authors have used these techniques to analyse the behaviour of individual components involved in mass loss reactions, leading to proposals of associated reaction mechanisms [5, 6].

The aim of the present study was to determine the thermal decomposition kinetics of granulated scrap tyres (GST) by TGA/DTG, and to compare the apparent activation energy ($E_a$) and the pre-exponential factor ($A$) values determined via the use of the Friedman, Flynn-Wall-Ozawa and Coats-Redfern model-free methods. Knowledge of these factors are important in the optimal design of industrial scale plants for GST recycling.

## 2. EXPERIMENTAL

### 2.1 Materials and Methods

The raw material used in this work was granulated scrap tyres (GST) obtained from a grinding and granulating plant (Negrell Residus, S.A., Banyoles, Gerona, Spain). This GST was largely composed of small particles (< 12 mm Ø) of natural and synthetic rubber compounds (63.5 %) and carbon black (32.4 %), plus a little fluff (< 2.0 wt.%) and steel (< 0.1 wt.%). Hydrocarbon oils (2.5 %), inorganic compounds (zinc oxide, sulphur and sulphur compounds) (1.6 %), stabilizers and anti-oxidants made up the rest [7].

Proximate and elemental analyses of the GST were performed using a Leco TGA 701 and Leco CHNS 923 analyser respectively. The GCV of the material was determined using an Ikaweeme C4000 automatic bomb calorimeter; analysis was performed on a ground sample previously frozen in liquid nitrogen.

### 2.2. Thermal decomposition and identification of temperature peaks

A representative sample of the GST was immersed in liquid nitrogen, ground and subjected to TGA. Thermal decomposition was achieved by heating a 40 mg sample in a 200 µl alumina crucible under an $N_2$ atmosphere (flow rate 20 ml/min), from room temperature to 650 ºC (heating

---

*Corresponding author. Tel.: +34-91-5538900, fax: +34-915347425.
E-mail address: *flopez@cenim.csic.es* (F. A. López)

rate 10 ºC/min) using a Setaram Sensys Evolution 1500 analyser.

The temperature peaks in the resulting thermogram were identified by performing control tests with pure NR, SBR and BR supplied by Jenecan S.A. (Bilbao, Spain).

## 2.3. Mathematical models for determining mass loss kinetics

The kinetic study of the decomposition of GST was performed by TGA/DTG using the same Setaram Sensys Evolution 1500 analyser. Given the thermal decomposition behaviour of the GST, non-isothermal analysis was performed between 230 ºC and 650 ºC at heating rates of 5, 10, 15, and 20 ºC/min, and the resulting thermograms recorded. Temperature calibration was performed using ICTAC-recommended standards. The accuracy of the reported temperatures was estimated to be ±2 ºC. The sample mass (about 60 mg) was placed in a 200 µl alumina crucible. All analyses were conducted in a $N_2$ atmosphere (flow rate 20 ml/min).

In rubber decomposition, it is generally assumed that the rate of conversion of the component polymers is proportional to the concentration (wt%) of the reacted material [8]. The rate of conversion can be expressed by the following basic rate equation (1):

$$\frac{d\alpha}{dt} = \beta\frac{d\alpha}{dT} = k(T)\cdot f(\alpha) \ , \quad (1)$$

where $\alpha$ is the degree of the advancement of the reaction, and $f(\alpha)$ and $k(T)$ are functions of conversion and temperature respectively. The degree of conversion $(\alpha)$ is calculated in terms of mass loss according to equation (2):

$$\alpha = \frac{w_0 - w_t}{w_0 - w_f} , \quad (2)$$

where $w_0$, $w_t$ and $w_f$ are the masses of the sample at the beginning of the decomposition process, the mass at any chosen point in the TG curve, and the final mass respectively. $k(T)$ is the temperature dependent on the rate of heat flow; this is often modelled successfully by the Arrhenius equation:

$$k(T) = Ae^{-E/RT} \ , \quad (3)$$

where $E$ (kJ/mol) is the activation energy, $A$ ($\text{min}^{-1}$) the pre-exponential factor, and $R$ (8.314 J/mol·K) the gas constant. By combining equations (1) and (3), the reaction rate can be written as follow:

$$\frac{d\alpha}{dt} = Ae^{-E/RT} f(\alpha) . \quad (4)$$

### 2.3.1. Mass loss kinetics as determined by the Friedman method

Friedman analysis [9], which is based on the Arrhenius equation, takes into account the logarithm of the conversion rate ($d\alpha/dt$) as a function of the reciprocal of the temperature (i.e., $1/T$) at different degrees of conversion α, according to equation:

$$\ln\frac{d\alpha}{dt}\,\Big|_{\alpha i} = \ln\left(A_i f(\alpha_{i,j})\right) - \frac{E_{ai}}{R\cdot T_{i,j}} , \quad (5)$$

where $i$ is the index of conversion, $j$ is the curve index, $E_a$ the apparent activation energy at $\alpha_i$, and $f(\alpha_{i,j})$ the function dependent on the reaction model (assumed to be constant for a given reaction progress $\alpha_{i,j}$ for all curves $j$). Since $f(\alpha)$ is constant at each degree of conversion $\alpha_i$, the curve for the logarithm of the reaction rate vs. $1/T$ is linear, with a slope of $E_a/R$ and an intercept $A$.

### 2.3.2. Mass loss kinetics as determined by the Flynn-Wall-Ozawa method

The Flynn-Wall-Ozawa method [10, 11] is derived from the integral isoconversional method. Using Doyle's approximation [12], the reaction rate in logarithmic form can be expressed as:

$$\ln\beta = \ln\left(\frac{AE_a}{R\cdot g(\alpha)}\right) - 5.331 - 1.052\frac{E_a}{R}\frac{1}{T} , \quad (6)$$

where $g(\alpha)$ is the function of conversion. Thus, for any constant α value, the plot $\ln\beta$ vs. $1/T$ recorded at different heating rates should be a straight line. The $E_a$ can be then determined from its slope.

### 2.3.3. Mass loss kinetics as determined by the Coats-Redfern method

The Coats-Redfern method [13] provides the thermal decomposition mechanism from the mass loss. An asymptotic approximation of $2RT/E_a < 1$ for the resolution of equation (7)

$$g(\alpha) = \int_0^{\alpha}\frac{d\alpha}{f(\alpha)} = \frac{A}{\beta}\int_{T_0}^{T}\exp\left(-\frac{E_a}{RT}\right)dT = \frac{AE_a}{\beta R}\,p\left(\frac{E_a}{RT}\right) \quad (7)$$

allows equation (8) to be obtained:

$$\ln\frac{g(\alpha)}{T^2} = \ln\frac{AR}{\beta E} - \frac{E_a}{RT} \quad (8)$$

The Coats-Redfern method is one of the most widely used procedures for the determination of reaction processes. The $E_a$ at a constant heating rate for any of the $g(\alpha)$ functions listed in Table 1 can be obtained from equation (8). Table 1 indicates the algebraic expressions of $f(\alpha)$ and $g(\alpha)$.

## 3. RESULTS AND DISCUSSION

Table 2 shows the results of the chemical analysis of the GST. High carbon (86 wt.%) and volatile compound (66 wt.%) contents were detected. The sulphur content (associated with vulcanisation) was an appreciable ~2 wt.%, the ash content ~5 wt.%, and the GCV ~38 MJ/kg.

### 3.1. Thermal decomposition of the GST

Figure 1 shows the initial TGA/DTG curve for GST at the 10 ºC/min heating rate used to determine its decomposition behaviour. Thermal decomposition started at about 290 ºC and was complete at 550 ºC.

**Table 1.** Algebraic expressions of functions of the most common reaction mechanisms

| Mechanism | $f(\alpha)$ | $g(\alpha)$ |
|---|---|---|
| Autocatalytic | $(1-\alpha)^n \cdot \alpha^m$ | – |
| Avarani-Erofe've (An) | $n(1-\alpha)\,[-\ln(1-\alpha)]^{(1-1/n)}$ | $[-\ln(1-\alpha)](1-1/n)$ |
| Avarani-Erofe've (A2) | $2(1-\alpha)\,[-\ln(1-\alpha)]^{1/2}$ | $[-\ln(1-\alpha)]^{1/2}$ |
| Avarani-Erofe've (A3) | $3(1-\alpha)\,[-\ln(1-\alpha)]^{2/3}$ | $[-\ln(1-\alpha)]^{1/3}$ |
| First-order (F1) | $(1-\alpha)$ | $-\ln(1-\alpha)$ |
| Second-order (F2) | $(1-\alpha)^2$ | $(1-\alpha)^{-1}-1$ |
| Third-order (F3) | $(1-\alpha)^3$ | $[(1-\alpha)^{-2}-1]/2$ |
| Contracting sphere (R2) | $2(1-\alpha)^{1/2}$ | $[1-(1-\alpha)^{1/2}]$ |
| Contracting Cylinder (R3) | $3(1-\alpha)^{2/3}$ | $[1-(1-\alpha)^{1/3}]$ |
| Power law (P2) | $2\alpha^{1/2}$ | $\alpha^{1/2}$ |
| Power law (P3) | $3\alpha^{1/3}$ | $\alpha^{1/3}$ |
| Power law (P4) | $4\alpha^{1/4}$ | $\alpha^{1/4}$ |
| One-dimensional diffusion (D1) | $1/2\alpha$ | $\alpha^2$ |
| Two-dimensional diffusion (D2) | $[-\ln(1-\alpha)]^{-1}$ | $[(1-\alpha)\cdot\ln(1-\alpha)]+\alpha$ |
| Three-dimensional diffusion (D3) | $3(1-\alpha)^{(2/3)}/2[(1-(1-\alpha)^{(1/3)})]$ | $[1-(1-\alpha)^{1/3}]^2$ |
| Giustling-Brounsthein (D4) | $1.5\,[(1-\alpha)^{(-1/3)}-1]$ | $1-(2\alpha/3)-(1-\alpha)^{2/3}$ |

Three consecutive phases can be distinguished: i) elimination of the oil and lubricants present in the GST ($T_m$ = 266.3 ºC), ii) breakdown of the NR ($T_m$ = 373.1 ºC), and iii) breakdown of the SBR and BR ($T_m$ = 435.6 ºC). The temperature profiles for the decomposition of the NR and SBR are similar to those of pure elastomers (Fig. 2). Thus the peak value observed at $T_m$ = 377.9 ºC for the decomposition of NR, those seen at $T_m$ = 425.4 ºC (styrene) and $T_m$ = 467.3 ºC (butadiene) for SBR, and that appearing at 467 ºC for BR, match those reported by other authors (NR 378 ºC, and SBR and BR 463 ºC [14]).

## 3.2. Kinetics of pyrolysis

Figure 3 shows the DTG curves for the decomposition of the GST at different heating rates (5 – 20 ºC/min) up to 650 ºC. Table 3 shows that higher heating rates result in an increase in peak temperatures and greater mass losses. The total mean mass loss was (61.7 ±6.5) wt.%, similar to the volatile compound content in GST (see Table 2).

### 3.2.1. Friedman method

The results of the DTG curves were first used to calculate the $E_a$ of pyrolysis of the GST via the Friedman method. The value of this variable was determined for different conversion values. The plot of the variation of $\ln(d\alpha/dt)$ against $1/T$, for a constant $f(\alpha)$ at each degree of conversion $\alpha_i$, produced a straight line for each $\alpha_i$ value, with a slope ($E_a/R$) (Fig. 4).

**Table 2.** Results of proximate and ultimate analyses of GST, and gross calorific value

| Variable | wt.% |
|---|---|
| Moisture (wt.% db) | 0.4 |
| Volatile matter (wt.% db) | 66.0 |
| Ash (wt.% db) | 4.9 |
| Fixed carbon (wt.% db) | 29.1 |
| C (wt.% daf) | 86.0 |
| H (wt.% daf) | 8.4 |
| N (wt.% daf) | 0.5 |
| S (wt.% daf) | 1.9 |
| $O^a$ (wt.% daf) | 3.2 |
| GCV (MJ/kg) | 38.3 |

Note. db – dry basis, daf – dry ash free; $^a$ calculated by difference.

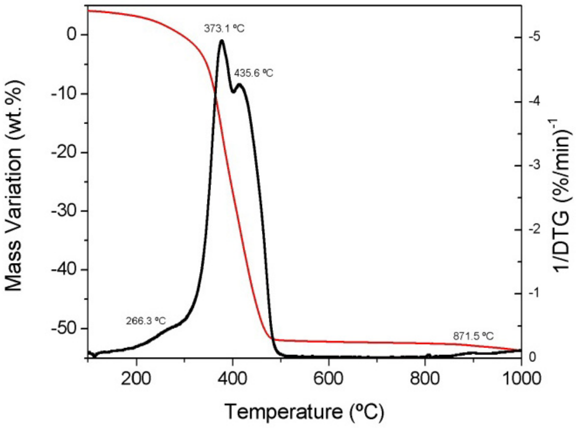

**Fig. 1.** TGA and DTG curves for the pyrolysis of GST

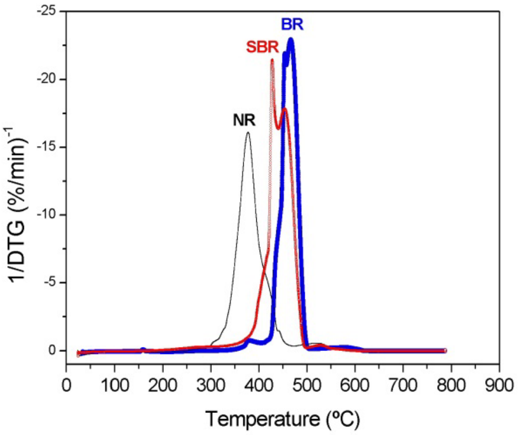

**Fig. 2.** DTG curves for the pyrolysis of pure elastomers

**Table 3.** TGA and DTG data for the pyrolysis of the granulated scrap tyres at different heating rates

| $\beta$ (ºC/min) | DTG | | TG | | |
|---|---|---|---|---|---|
| | Peak 1 $T_m$ (ºC) | Peak 2 $T_m$ (ºC) | Peak 1 weight loss (wt. %) | Peak 2 weight loss (wt.%) | Total weight loss (wt.%) |
| 5 | 365 | 443 | 20.55 | 36.60 | 57.15 |
| 10 | 373 | 436 | 29.04 | 25.81 | 54.85 |
| 15 | 385 | 444 | 39.11 | 26.94 | 66.05 |
| 20 | 389 | 472 | 30.58 | 37.88 | 68.46 |

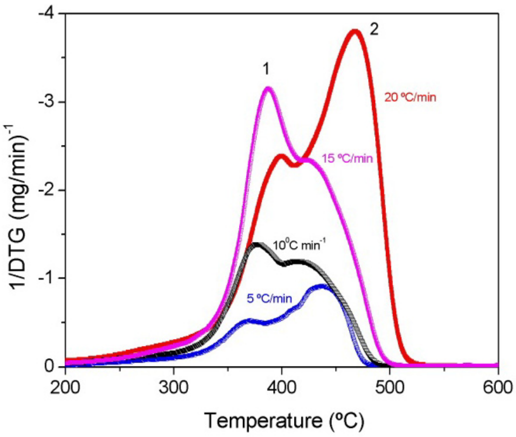

**Fig. 3.** DTG curves for the decomposition of granulated scrap tyres at different heating rates

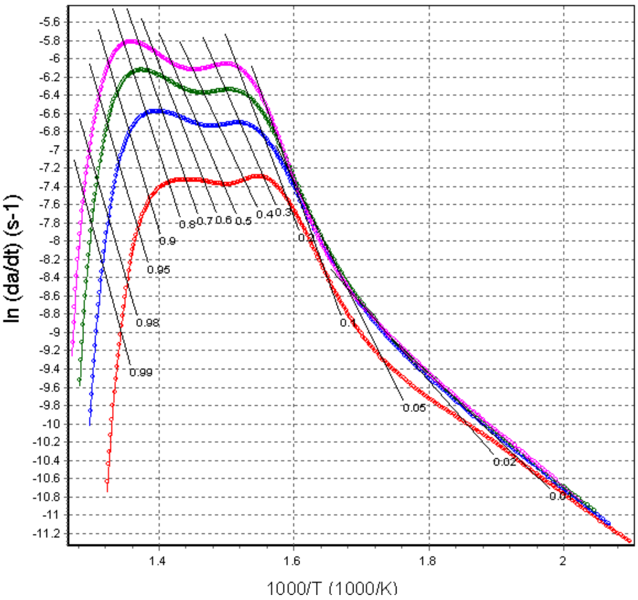

**Fig. 4.** Kinetics for the pyrolysis of granulated scrap tyre as determined by the Friedman method

Figure 5 shows the changes in $E_a$ according to the degree of conversion, for the overall pyrolysis of the GST. Four stages characterized by different $E_a$ values can be seen. In the first stage ($0.01 \leq \alpha \leq 0.12$), $E_a$ increases from 120 kJ/mol to 175.5 kJ/mol, with a mean of 155.9 kJ/mol ±15.7 kJ/mol. In the second stage ($0.12 \leq \alpha \leq 0.38$), the $E_a$ falls as low as 132 kJ/mol (mean 152.9 kJ/mol ±15.4 kJ/mol). In the third stage there is a long $\alpha$ interval ($0.38 \leq \alpha \leq 0.90$), during which $E_a$ reaches as high as 206.6 kJ/mol (mean 167.1 kJ/mol ±2.4 kJ/mol). Finally, in the fourth stage ($0.90 \leq \alpha \leq 0.998$), the $E_a$ varies from 206 kJ/mol to 209 kJ/mol (mean $E_a$ 207.3 kJ/mol ±0.8 kJ/mol). The mean $E_a$ obtained in the ($0.01 \leq \alpha \leq 1$) interval was 166.0 kJ/mol ±12.7 kJ/mol and the pre-exponential factor ($A$) was $1.24 \cdot 10^{10}$ $s^{-1}$. The existence of four stages suggests the mechanism of decomposition is similar to that proposed by Seneca et al. [6] for the pyrolysis of scrap tyres.

Figure 6 also shows the changes in the slope over different parts of the $E_a$ variation curve, for which the coefficient of linear regression ($R^2$) values can be calculated.

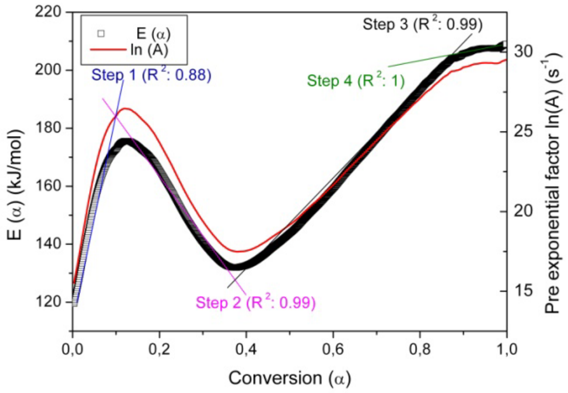

**Fig. 5.** Apparent activation energy, as determined by the Friedman method

### 3.2.2. Flynn-Wall-Ozawa method

Using equation (6), the $E_a$ of the GST was obtained from the plot ln($\beta$) vs. $1/T$ for a fixed degree of conversion; the slope was $1.052\,E_a/R$ (Fig. 6). The mean $E_a$ was 167.7 kJ/mol ±17.2 kJ/mol for the interval ($0 \leq \alpha \leq 1$). Thus, the values for $E_a$ are similar when calculated using either the Friedman (166 kJ/mol) or Flynn-Wall-Ozawa (167.7 kJ/mol) methods.

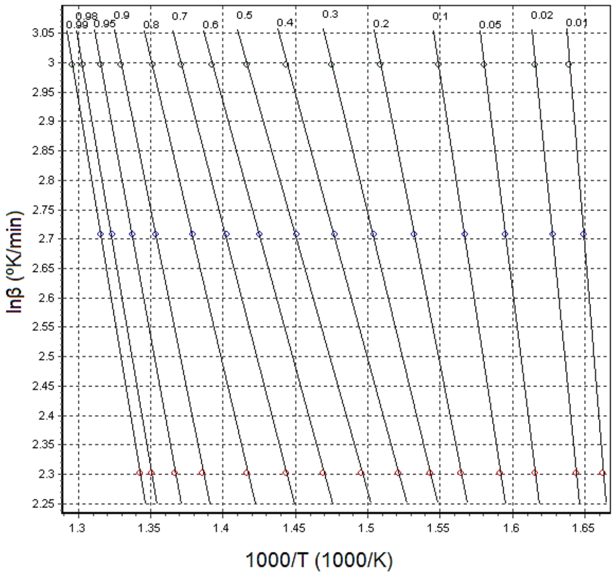

**Fig. 6.** Variation in ln($\beta$) vs. $1/T$ for different $\alpha$ values (Flynn-Wall-Ozawa plot)

### 3.2.3. Coats-Redfern method

Table 4 shows the different $E_a$ values for differing $f(\alpha)$ values, as determined by the Coats-Redfern method, for a constant heating rate of 10 ºC/min. The $E_a$ value most similar to those returned by the Friedman (166 kJ/mol) and Flynn-Wall-Ozawa (167.7 kJ/mol) methods, was 160 kJ/mol, while the $A$ value was $4.15 \cdot 10^{8}$ $s^{-1}$. These values correspond to a three-dimensional diffusion (D3) model.

Thus, the $E_a$ calculated from the global reaction (peak 1 and peak 2 in the DTG plots) varies depending on the calculation method used, from 160 kJ/mol to 167.7 kJ/mol.

A discrepancy is seen, however, between the $A$ Friedman ($1.24 \cdot 10^{10}$ $s^{-1}$) and $A$ Coats-Redfern ($4.15 \cdot 10^{8}$ $s^{-1}$) values.

**Table 4**. Activation energies, pre-exponential factors and order of reaction of pyrolysis of GST as determined by the Coats-Redfern method

| Mechanism | $A$ ($s^{-1}$) | $E$ (kJ/mol) | n | m |
|---|---|---|---|---|
| D3 | $4.15\times10^{8}$ | 160.00 | – | – |
| Autocatalytic | $4.5\times10^{7}$ | 136.93 | 0.933 | 0.648 |
| An | $7.01\times10^{7}$ | 134.77 | 0.698 | – |
| Fn | $1.49\times10^{4}$ | 88.277 | 0.872 | – |
| Rn | $1.91\times10^{3}$ | 88.277 | 7.82 | – |
| F1 | $5.81\times10^{4}$ | 95.26 | 1 | – |
| R3 | $5.59\times10^{2}$ | 77.07 | 3 | – |
| A1.5 | $2.17\times10^{2}$ | 64.82 | 1.5 | – |
| D4 | $1.2\times10^{7}$ | 141.81 | – | – |
| R2 | $1.42\times10^{2}$ | 67.971 | 2 | – |
| A2 | $1.21\times10^{2}$ | 49.60 | 2 | – |
| D2 | $7.99\times10^{6}$ | 132.01 | – | – |
| Pn | $3.44\times10^{1}$ | 58.99 | 0.793 | – |
| P1 | 1.39 | 40.69 | 1 | – |
| D1 | $2.4\times10^{5}$ | 110.64 | – | – |
| P2 | $2.37\times10^{-3}$ | 57.12 | 2 | – |
| P3 | $2.38\times10^{-4}$ | –5.95 | 3 | – |
| P4 | $6.92\times10^{-5}$ | –11.78 | 4 | – |
| F2 | $2.43\times10^{9}$ | 149.82 | 2 | – |
| F3 | $1.01\times10^{14}$ | 204.39 | 3 | – |

Discrepancies were seen between the $E_a$ and $A$ values obtained and the many different values for these variables reported by other authors (Table 5). This is in part explained by the different kinetic models used in their calculation, but also to likely variation in the types of scrap tyre examined (car, truck, agricultural vehicle and motorcycle tyres, etc.). There are many different manufacturers and countless different formulations used around the world; the composition of the tyre varies depending on the tyre grade and manufacturer. Consequently, tyre thermal degradation or pyrolysis products may also vary in terms of yield and chemical composition. Different tyres have different proportions of SBR, NR and BR, and would therefore return different $E_a$ values: for example, Yang et al. [17] reported values of 152 kJ/mol for pure SBR, 207 kJ/mol for NR and 215 kJ/mol for BR. In addition, Ucar et al. [22], who determined the polymer types in the rubber content of scrap truck and car tyre wastes, reported truck tyre waste to contain 51 wt.% NR, 39 wt.% SBR and 10 wt.% BR, while car tyre waste contained 35 wt.% NR and 65 wt.% BR. They also found significant variation in terms of kinetic variables and proximate and ultimate analysis results for these types of waste, as well as variations in pyrolytic product yields and liquid and gaseous product compositions.

Kyari et al. [23] and Islam et al. [24] studied the pyrolysis of seven brands of used car tyres from several countries, and characterized the liquid products obtained after individual type and mixed pyrolysis. Significant variation was seen in terms of the concentration of different compounds in the derived liquid and gaseous products. In the present work, the GST, which was a mixture of all types of tyre, returned an $E_a$ close to that for pure SBR reported by Yang et al. [17]. This suggests that the present GST was very rich in SBR.

**Table 5.** Kinetic values for the pyrolysis of granulated scrap tyres

| Reference | Activation Energy, $E$ (kJ/mol) | Pre-exponential factor, $A$ ($min^{-1}$) | Material |
|---|---|---|---|
| Present paper | 160 | $2.49\times10^{10}$ | Granulated Scrap tyre |
| Singh et al. [15] | 80 – 95.3 | – | Scrap tyre |
| Chen and Yeh [16] | 153 – 211 | $5.75\times10^{8}$ – $1.3\times10^{14}$ | SBR |
| Yang et al. [17] | 152<br>207<br>215 | $4.5\times10^{10}$<br>$2.36\times10^{16}$<br>$6.32\times10^{14}$ | SBR<br>NR<br>R |
| Leung and Wang [18] | 164.5 – 218.7 | $6.29\times10^{13}$ – $1.13\times10^{17}$ | Tyre powder |
| Haydary et al. [19] | 96 – 105 | $1.52\times10^{6}$ – $6.84\times10^{6}$ | Scrap tyre |
| Aylon et al. [20] | 70 – 256 | – | Scrap tyre |
| Lopez et al. [21] | 50.6 – 246 | $1.47\times10^{3}$ – $4.86\times10^{18}$ | Scrap tyre (Vacuum pyrolysis at 1 atm) |

The kinetic equations for GST pyrolysis are as follows:

$$\frac{d\alpha}{dt} = 4.15\times10^{8} e^{-160/RT} \cdot f(\alpha), \tag{9}$$

where $f(\alpha)$ can be written as follow:

$$f(\alpha) = 3(1-\alpha)^{(2/3)}/[2(1-(1-\alpha)^{(1/3)})]. \tag{10}$$

## 4. CONCLUSIONS

The thermal degradation kinetics of GST were investigated thermogravimetrically for heating rates of 5, 10, 15 and 20 ºC/min and a temperature range of 230 ºC – 650 ºC with nitrogen as the carrier gas. The results show that thermal decomposition starts at about 290ºC and is complete at 550 ºC. The reaction begins with the dehydration and decomposition of the processing oils, followed by the decomposition of the NR and/or BR. The rate equation for GST can be modelled satisfactorily by a simple reaction. The average $E_a$ and $A$ values for the GST were 160 kJ/mol and $2.49\times10^{10}$ $min^{-1}$ respectively.

The mean $E_a$ values obtained by the different model-free methods used were similar. The thermal decomposition reaction model, as determined by the Coats-Redfern method, is accounted for by the D3 model. The $E_a$ was found not to be constant over the $\alpha$ interval 0.01 – 0.99, suggesting that the pyrolysis of GST is a multi-step process. A discrepancy was seen in the A values as determined by the Friedman and the Flynn-Wall-Ozawa methods. Knowledge of the $E_a$ and $A$ values, and of the kinetic model that describes the pyrolysis of GST, are important for the optimal design of industrial scale GST recycling plants.

## *Acknowledgements*

This research was funded by ENRECO 2000 Ltd.

## Nomenclature

TGA: Thermogravimetry analysis
DTG: Differential thermogravimetry
$E$: Activation energy [kJ/mol]
$E_a$: Apparent activation energy at α [kJ/mol]
$A$: Pre-exponential factor [$s^{-1}$]
$\alpha$: conversion [-]
$w_0$: initial mass[g]
$w_t$: actual mass [g]
$w_f$: final mass [g]
n and m: reaction order [–]
$R$: gas constant [J/mol.K]
$T$: Temperature [ºC]
$T_m$: Maximum temperature peak [ºC]
$\beta$: Heating rate [K/min$^{-1}$]
$f(\alpha)$: Functions of conversion
$g(\alpha)$: Integral function of conversion
$R^2$: Linear regression.

## REFERENCES

1. European Tyre and Rubber Industry. Statistics. Edition 2012. http://www.etrma.org/uploads/ Modules/ Documentsmanager/20121119-etrma-statistics-2012.pdf
2. **López, F. A., Centeno, T. A., Alguacil, F. J., Lobato, B.** Distillation of Granulated Scrap Tires in a Pilot Plant *Journal of Hazardous Materials* 190 (1 – 3) 2011: pp. 285 – 292. http://dx.doi.org/10.1016/j.jhazmat.2011.03.039.
3. **Kardnkeyan, S., Sathiskumar, C., Moorthy, R. S.** Effect of Process Parameters on Tire Pyrolysis: a Review *Journal of Scientific & Industrial Research* 71 (5) 2012: pp. 309 – 315. http://nopr.niscair.res.in/handle/123456789/13986 doi:10.1016/s0165-2370(99)00017-0.
4. **Luyima, A., Zhang, L., Kers, J., Laurmaa, V.** Recovery of Metallic Materials from Printed Wiring Boards by Green Pyrolysis Process *Materials Science-Medziagotyra* 18 (3) 2012: pp.238 – 242. http://dx.doi.org/10.5755/j01.ms.18.3.2432.
5. **Al-Salem, S. M., Lettieri, P., Baeyens, J.** Kinetics and Product Distribution of End of Life Tyres (ELTs) Pyrolysis: a Novel Approach in Polyisoprene and SBR Thermal Cracking *Journal of Hazardous Materials* 172 (2 – 3) 2009: pp.1690 – 1694. http://dx.doi.org/10.1016/j.jhazmat.2009.07.127.
6. **Sennecaa, O., Salatino, P., Chironeb, R.** A Fast Heating-rate Thermogravimetric Study of the Pyrolysis of Scrap Tyres *Fuel* 78 (13) 1999: pp. 1575 – 1581. http://dx.doi.org/10.1016/S0016-2361(99)00087-3.
7. **López, F. A., Centeno, T. A., Alguacil, F. J., Lobato, B., López-Delgado, A., Fermoso, J.** Gasification of the Char Derived from Distillation of Granulated Scrap Tyres *Waste Management* 32 2012: pp. 743 – 752. http://dx.doi.org/10.1016/j.wasman.2011.08.006
8. **Mohoriè, I., Krajnc, M., Šebenikb, U.** Model-free Kinetics Analysis of Thermal Degradation of Polysiloxane Lubricant *Chemical and Biochemical Engineering Quartherly* 23 (4) 2009: pp.493 – 496. http://pierre.fkit.hr/hdki/cabeq/pdf/23_4_2009/Cabeq_2009_04_11.pdf
9. **Friedman, H. L.** Kinetics of Thermal Degradation of Char-forming Plastics from Thermogravimetry. Application to a Phenolic Plastic *Journal of Polymer Science Part C* 6 (1) 1964: pp. 183 – 195. doi: 10.1002/polc.5070060121.
10. **Flynn, J., Wall, L.** A Quick, Direct Method for the Determination of Activation Energy from Thermogravimetric Data *Journal of Polymer Science Part B: Polymer Letters* 4 (5) 1966: pp.4323 – 328. doi: 10.1002/pol.1966.110040504.
11. **Ozawa, A.** New Method of Analyzing Thermogravimetric Data *Bulletin of Chemical Society of Japan* 38 (11) 1965: pp.1881 – 1886. doi:10.1246/bcsj.38.1881.
12. **Doyle, C.** Kinetic Analysis of Thermogravimetric Data *Journal of Applied Polymers Science* 5 (15) 1961: pp. 285 – 292. doi:10.1002/app.1961.070051506.
13. **Coats, A. W., Redfern, J. P.** Kinetic Parameters from Thermogravimetric Data *Nature* 201 1964: pp. 68 – 69. doi:10.1038/201068a0.
14. **Galvagno, S., Casu, A., Martino, M., Di Palma, E., Portofino, S.** Thermal and Kinetic Study of Tyre Waste Pyrolysis via TG-FTIR-MS Analysis *Journal of Thermal Analysis and Calorimetry* 88 (2) 2007: pp. 507 – 514. http://dx.doi.org/10.1007/s10973-006-8409-1.
15. **Singh, S., Wu, C., Williams, P. T.** Pyrolysis of Waste Materials Using TGA-MS and TGA-FTIR as Complementary Characterisation Techniques *Journal of Analytical and Applied Pyrolysis* 94 2012: pp. 99 – 107. http://dx.doi.org/10.1016/j.jaap.2011.11.011
16. **Chen, K. S., Yen, R. Z.** Kinetics of Thermal Decomposition of Styrene Butadiene Rubber at Low Heating Rates in Nitrogen and Oxygen *Combustion and Flame* 180 1997 pp. 408 – 418. http://dx.doi.org/10.1016/S0010-2180(96)00142-3
17. **Yang, J., Kaliaguine, S., Roy, C.,** Improved Quantitative Determination of Elastomers in Tyre Rubber by Kinetic Simulation of DTG Curves, *Rubber Chemistry and Technology* 66 (2) 1993: pp. 213 – 229. http://dx.doi.org/10.5254/1.3538307
18. **Leung, D. Y. C., Wang, C. L.** Kinetic Study of Scrap Tyre Pyrolysis and Combustion *Journal of Analytical and Applied Pyrolysis* 45 (2) 1998: pp. 153 – 169. http://dx.doi.org/10.1016/S0165-2370(98)00065-5
19. **Haydary, J., Koreňová, Z., Jelemenský, L., Markoš, J.** Thermal Decomposition of Waste Polymers *THERMOPHYSICS 2008* October 16 and 17, 2008, Kočovce, Slovakia. Editors: Jozef Leja & Slávka Prváková, Vydavateľstvo STU, Bratislava 2008: pp.16 – 17. ISBN 978-80-227-2968-0. http://www.tpl.fpv.ukf.sk/engl_vers/thermophys/2008/documents/Haydary.pdf
20. **Aylon, E., Callen, M. S., Lopez, J. M., Mastral, A. M., Murillo, R., Navarro, M. V., Stelmach, S.** Assessment of Tire Devolatilization Kinetics *Journal of Analytical and Applied Pyrolysis* 74 2005: pp. 259 – 264. http://dx.doi.org/10.1016/j.jaap.2004.09.006
21. **Lopez, G., Aguado, R., Olazar, M., Arabiourrutia, M., Bilbao, J.** Kinetics of Scrap Tyre Pyrolysis under Vacuum Conditions *Waste Management* 29 (10) 2009: pp. 2649 – 2655. http://dx.doi.org/10.1016/j.wasman.2009.06.005
22. **Ucar, S., Karagoz, S., Ozkan, A. R., Yanik, J.** Evaluation of Two Different Scrap Tires as Hydrocarbon Source by Pyrolysis *Fuel* 84 2005: pp. 1884 – 1892. http://dx.doi.org/10.1016/j.fuel.2005.04.002
23. **Kyari, M., Cunliffe, A., Williams, P. T.** Characterization of Oils, Gases, and Char in Relation to the Pyrolysis of Different Brands of Scrap Automotive Tires *Energy and Fuels* 19 (3) 2005: pp. 1165 – 1173. doi: 10.1021/ef049686x
24. **Islam, M. R., Haniu, H., Rafiqul Alam Beg, M.** Liquid Fuels and Chemicals from Pyrolysis of Motorcycle Tire Waste: Product Yields, Compositions and Related Properties *Fuel* 87 (13 – 14) 2008: pp. 3112 – 3122. http://dx.doi.org/10.1016/j.fuel.2008.04.036